ACS chemical biology

Letters

pubs.acs.org/acschemicalbiology

Terms of Use CC-BY

Crystal Structures of Stapled and Hydrogen Bond Surrogate Peptides Targeting a Fully Buried Protein−Helix Interaction

Christopher H. Douse,[†,‡,§] Sabrina J. Maas,[†] Jemima C. Thomas,[†,⊥] James A. Garnett,[‡] Yunyun Sun,[†,§] Ernesto Cota,*[,‡,§] and Edward W. Tate*[,†,§]

[†]Department of Chemistry, [‡]Centre for Structural Biology, Department of Life Sciences, and [§]Institute of Chemical Biology, Imperial College London, London SW7 2AZ, United Kingdom

Supporting Information

ABSTRACT: Constrained α-helical peptides are an exciting class of molecule designed to disrupt protein−protein interactions (PPIs) at a surface-exposed helix binding site. Complexes that engage more than one helical face account for over a third of structurally characterized helix PPIs, including several examples where the helix is fully buried. However, no constrained peptides have been reported that have targeted this class of interaction. We report the design of stapled and hydrogen bond surrogate (HBS) peptides mimicking the helical tail of the malaria parasite invasion motor myosin (myoA), which presents polar and hydrophobic functionality on all three faces in binding its partner, myoA tail interacting protein (MTIP), with high affinity. The first structures of these different constrained peptides bound to the same target are reported, enabling a direct comparison between these constraints and between staples based on monosubstituted pentenyl glycine (pGly) and disubstituted pentenyl alanine (pAla). Importantly, installation of these constraints does not disrupt native interactions in the buried site, so the affinity of the wild-type peptide is maintained.

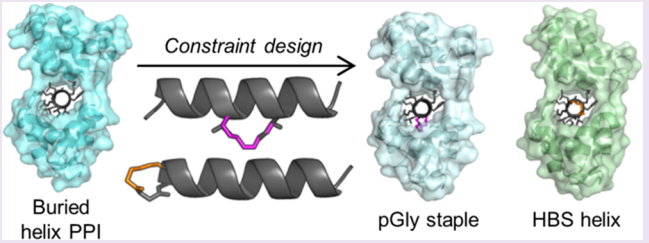

Protein−protein interactions (PPIs) mediated through an α-helix represent an important class of potential therapeutic targets, and there is ongoing interest in the use of synthetic methods to mimic and/or constrain the conformational flexibility of helical peptides to improve binding affinity for a receptor, increase proteolytic stability, or enhance cell penetration.[1] The most prominent examples of such strategies include "hydrogen bond surrogate" (HBS) helices and stapled peptides (Figure 1a).[2,3] The former feature replacement of one intramolecular i to i+4 main chain hydrogen bond by a covalent bond at the N-terminus of the peptide, while the latter are typically constrained through hydrophobic linkers established by ring-closing metathesis between α,α-disubstituted alkenyl alanine residues positioned at appropriate positions along the sequence. Among several examples that highlight the potential of these approaches, a HBS helix was recently shown to regulate hypoxia-inducible genes important for cancer progression via modulation of the interaction between HIF-1α with coactivator p300,[4] and a stapled dual inhibitor of the p53-Mdm2/MdmX interactions showed encouraging tumor suppression in models of human osteosarcoma and breast cancer.[5] The applicability of constrained peptides has so far been mostly limited to surface-exposed PPIs dominated by hydrophobic interactions; however, more than a third of structurally characterized protein−helix interactions are buried, with two or all three faces of the helix presenting "hotspot" residues.[6,7] Two faces have been exploited by stapled coactivator peptides targeting estrogen receptors, although stapling at one position caused a change in helix register.[8] Fully buried complexes represent an unprecedented and highly challenging target for constrained peptides, since any constraining motif must preserve the array of native interactions by design. Several X-ray crystal structures of stapled peptide complexes have been reported, showing that the staple may unexpectedly engage in interactions with hydrophobic sites on the receptor protein,[5,8−10] while the mode of recognition of a HBS helix has yet to be described in atomic detail. When targeting a buried PPI, association of the constraint with the protein is a primary design consideration since it must not perturb hotspot side chain orientations or change the register of the helix.

We sought to address these challenges by making the first comparison of stapling and HBS technologies directed against the same target protein using a fully buried helix PPI, *Plasmodium falciparum* myosin A (myoA)−myoA tail interacting protein (MTIP), as a template. In the human malaria parasite, myoA couples ATP hydrolysis to overall motility and drives invasion of host red blood cells; interaction with MTIP defines its intracellular localization.[11,12] Constrained, stabilized myoA tail peptides could represent useful tool molecules to enable investigation of myoA-based motility in the malaria parasite via replacement of the native myosin in this complex, without recourse to altering the parasite at the genetic level. Unmodified peptides from the wild-type (WT) myoA tail have produced variable results in such experiments,[13,14] suggesting

Received: April 12, 2014
Accepted: August 1, 2014
Published: August 1, 2014

 © 2014 American Chemical Society

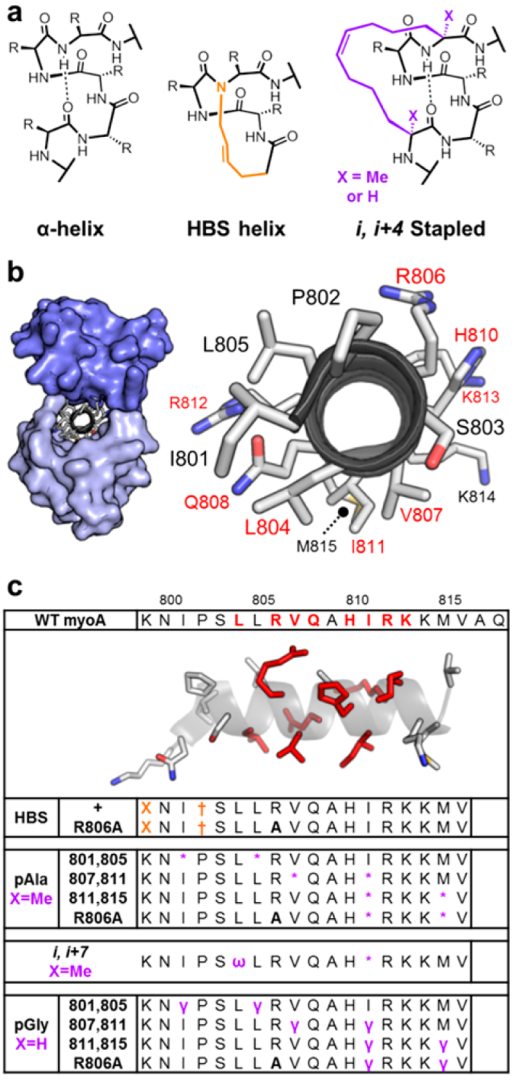

Figure 1. (a) Schematic diagrams of α-helix constraints used in this study. (b) Archetypal buried protein–helix interaction MTIP-myoA tail from *P. falciparum* with two MTIP domains (surface) "clamped" around myoA. Close-up of the myoA helix (gray cartoon) showing that hotspot residues (red) are found on all faces. (c) Library of constrained myoA tail peptides. Shown are the sequences before ring-closing metathesis, with X = (4′)-pentenoic acid; † = *N*-allyl glycine; * = (*S*)-pentenyl alanine; ω = (*R*)-octenyl alanine; γ = (*S*)-pentenyl glycine.

that their stability and cell penetrating capacity require improvement. MTIP features two linked myoA-binding domains that are highly flexible in isolation; on binding these domains form a rigid, enthalpy-dominated "clamp" around the helical myoA tail, burying >2000 Å^2 of surface area in so doing. According to crystal structures of the complex, a number of polar and nonpolar hotspot residues are displayed on all sides of the myoA helix (Figure 1b).[14−16] Since the wild-type (WT) myoA tail binds with high affinity in this congested binding groove,[16] it was critical that the constraint introduction did not interfere with the native MTIP-myoA contacts.

With this point in mind, we first designed and synthesized a library of modified myoA tail peptides (Figure 1c) to compare the HBS approach and staples based on widely used disubstituted alkenyl alanine derivatives. Positions for unnatural motifs were selected on the basis of analysis of the WT complex (PDB entry: 4AOM) and our understanding of the key determinants of binding.[14,16] The final C-terminal residues (Ala817 and Gln818) of WT myoA were removed since they are dispensable for a tight interaction.[14] We chose Pro802 and Lys799 for replacement by the HBS constraint because this region lies outside the buried interface and neither residue makes hotspot interactions with MTIP. For the stapled peptides, we replaced pairs of nonpolar WT myoA residues aiming to recreate or even enhance native hydrophobic interactions without perturbing key polar interactions and to test stapling across sequential turns of the helix. A myoA point mutation (R806A) was used in negative control peptides; Arg806 interacts with the interdomain linker and N-terminal domain of MTIP and templates the clamp around myoA, so peptides bearing this mutation display lower affinity than the WT sequence.[14,15]

The potential of these molecules to stabilize MTIP and disrupt the MTIP-myoA complex was investigated using differential scanning fluorimetry (DSF) and a FRET inhibition assay, respectively (Table 1). In the latter experiment, MTIP

Table 1. Biophysical Characterization of Constrained myoA Tail Peptides by DSF[a] and FRET

	ΔT_m (°C)	FRET IC_{50} (μM)
WT myoA	19.3 ± 0.9	4.4 ± 0.7
HBS myoA	16.1 ± 0.8	2.4 ± 0.3
HBS myoA R806A	13.0 ± 0.7	>100
pAla[801,805]	14.2 ± 1.4	8.0 ± 2.2
pGly[801,805]	25.9 ± 0.2	1.6 ± 0.4
pAla[807,811]	15.9 ± 1.1	10.0 ± 2.6
pGly[807,811]	19.3 ± 0.4	4.9 ± 1.6
pAla[811,815]	16.2 ± 0.9	4.3 ± 0.8
pGly[811,815]	16.3 ± 0.8	10.6 ± 2.7
pAla R806A	12.5 ± 1.0	>100
pGly R806A	10.3 ± 0.8	>100
i, *i*+7 staple	9.8 ± 0.4	9.8 ± 4.1

[a] T_m of MTIP Δ60 is 38.3 ± 0.2

residue Trp171 (located close in space to the N-terminal end of the myoA tail) was excited at 280 nm in a MTIP/dansyl-myoA tail peptide complex causing FRET to the dansyl group, which emits at 525 nm. Monitoring the drop in this signal due to displacement of the dansylated probe by competitive myoA peptides enabled determination of IC_{50} values (Supplementary Figures S1 and S2). We observed a relatively poor correlation between T_m shift (Supplementary Figure S3) and inhibitory potential, likely due in part to variations in assay conditions but also perhaps to the domain structure of the protein. For example, R806A controls display low potency since the MTIP clamp does not form but still stabilize the C-terminal domain, resulting in a substantial T_m shift (albeit with a shallower, less cooperative unfolding transition). Nonetheless, ^{1}H,^{15}N HSQC spectra (Supplementary Figure S4) of ^{15}N-labeled MTIP bound to the constrained peptides coupled with strongly diminished binding of R806A controls (IC_{50} > 100 μM in all cases) suggested that the designed peptides bound in a similar mode to WT myoA.

HBS myoA showed comparable potency (IC_{50} = 2.4 μM) to that of WT myoA (IC_{50} = 4.4 μM), as may have been expected given that the constraint was intentionally positioned across a part of the myoA tail outside the congested MTIP binding site. The ΔT_m was lower for this peptide (+16.1°, cf. +19.3° for WT

dx.doi.org/10.1021/cb500271c | *ACS Chem. Biol.* 2014, 9, 2204−2209

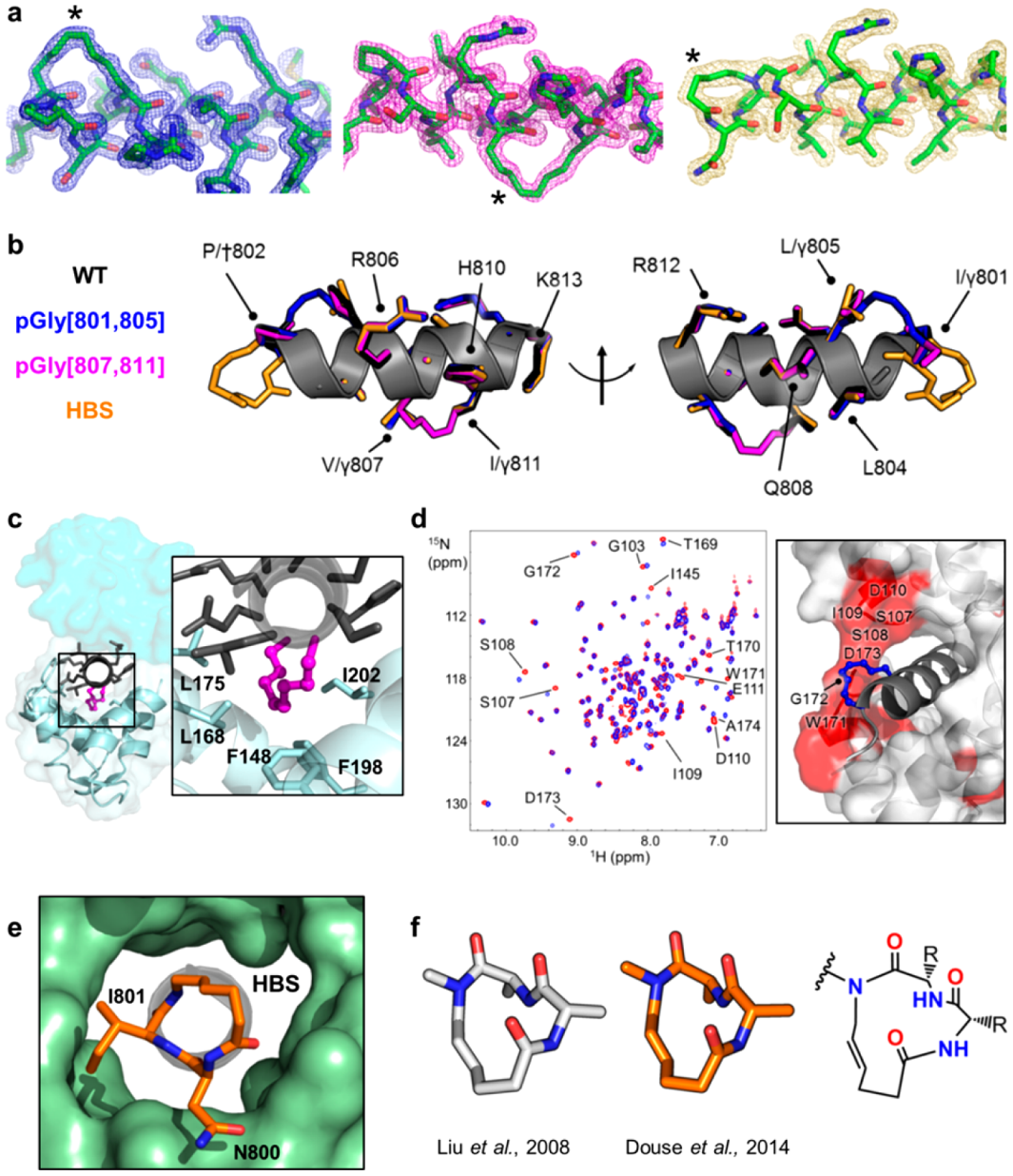

Figure 2. Structures of constrained myoA tail peptides in complex with myoA tail interacting protein (MTIP). (a) Refined $2F_o - F_c$ electron density maps of the three peptides bound to MTIP, contoured at 1.5σ (constraints marked with an asterisk). (b) Comparison of the helices (gray cartoon) formed by different peptides in complex with MTIP: the native myoA tail (side chains in black, PDB entry 4AOM) and three constrained peptides (pGly[801,805] side chains in blue; pGly[807,811] in magenta; HBS myoA in orange, respectively; PDB entries 4MZJ, 4MZK, and 4MZL). (c) X-ray structure of MTIP bound to pGly[807,811] viewed down the myoA tail helix (gray) from the N-terminus; the placement of the pGly staple (magenta spheres) in the center of the helix allows the aliphatic chain to plug into the small hydrophobic core of the MTIP C-terminal domain (inset). (d) Solution ^{1}H,^{15}N HSQC spectra of uniformly ^{15}N-labeled MTIP in complex with the WT myoA tail (red contours) and pGly[801,805] (blue). Residues whose backbone amide resonances are perturbed are highlighted in red on the adjacent X-ray structure (pGly staple shown as blue spheres). (e) The hydrogen bond surrogate (HBS) motif is positioned at the N-terminus of the myoA peptide and avoids steric clashes in the myoA binding groove. (f) Comparison of the HBS constraint in the crystal structures of an isolated HBS helix (CCDC entry 675526, left; white sticks; side chains removed for clarity) and HBS myoA bound to MTIP (center; orange), together with the chemical structure (right).

myoA), but the DSF transition was notably sharper, indicating a well-folded complex with high cooperativity of unfolding. In contrast, we observed a decrease in ΔT_m, the cooperativity of unfolding and potency upon introduction of two distinct *i*, *i*+4 pentenyl alanine stapling motifs (pAla[801,805] and pAla-[807,811]) or a longer *i*, *i*+7 staple, while pAla[811,815] was better tolerated. The clamped MTIP-myoA binding interface is sterically congested, and we considered that the α-methyl groups in the disubstituted pAla staples could adversely affect complex stability. A recent report on a peptide stapled through monosubstituted pentenyl glycine (pGly) suggests no significant differences from pAla in terms of helix stability or potency, but this peptide was designed to target a surface-exposed binding site,[17] and we hypothesized that the substitution pattern at Cα may become more important when targeting a buried protein−helix interaction. To this end, (*S*)-*N*-Fmoc pentenyl glycine (pGly) was synthesized using a nickel-based chiral auxiliary and incorporated in the myoA tail sequence in a

dx.doi.org/10.1021/cb500271c | ACS Chem. Biol. 2014, 9, 2204−2209

series of analogues using the same *i*, *i*+4 spacing as for the pAla series. Ring-closing metathesis on resin-bound peptides yielded ~8:2 mixtures of two products with the desired mass but different HPLC retention times. This was consistent with observations made by Blackwell and Grubbs using *O*-allyl serine-derived macrocycles,[18] but was in contrast to pAla staples where a single product was obtained and pGly stapling in other systems, where isomerism was not reported.[17,19]

The major and minor products were assigned as *cis* and *trans* alkenes, respectively, following HPLC separation of a control peptide and characterization by ^{1}H NMR. Circular dichroism (CD) spectroscopy showed that the *cis* staple conferred greater helicity than the *trans* isomer (Supplementary Figure S5). Notably, pGly[801,805] and pGly[807,811] displayed improved MTIP binding over their pAla analogues as measured by DSF and FRET, with pGly[801,805] displaying the highest potency (IC_{50} = 1.6 μM) and ΔT_m (+25.9°) across the whole library.

To explore the binding mode of the constraining motifs and understand these effects in atomic detail, we sought to co-crystallize the peptides with MTIP. Screening and optimization yielded diffraction-quality crystals for three of the four most promising analogues (pGly[801,805], pGly[807,811], and HBS myoA), and data sets were collected that permitted solution of the structures to resolutions of 1.47, 1.82, and 2.01 Å, respectively (Figure 2a and Supplementary Table S1).

Our design of the constraints was validated by several key features of these structures when compared to the WT structure: (i) the fold of MTIP is maintained with the two domains clamped around the constrained myoA peptides; (ii) the side chains of all key hotspot residues coincide nearly exactly between the structures, with RMSDs compared to WT of 0.11, 0.13, and 0.17 Å respectively; and (iii) the pGly staples follow the same trajectory as the hydrophobic residues that were replaced (Figure 2b). The latter point is particularly striking for the pGly[807,811] structure, in which the staple exactly tracks the bond vectors of the Val807 and Ile811 side chains and is effectively incorporated into the hydrophobic core of the MTIP C-terminal domain (Figure 2b and c). This structure is the first of a stapled peptide designed to occupy a deeply buried α-helix binding site. The co-crystal structure of MTIP and pGly[801,805] was corroborated by solution NMR analysis of the complex, providing a plausible explanation for this peptide's small increase in potency and very large ΔT_m. The HSQC spectrum showed chemical shift perturbations in localized regions of MTIP when overlaid with that of the WT complex, suggesting contacts made by the staple consistent with our design strategy. While hydrophobic interactions made by WT residues Ile801 and Leu805 are maintained in pGly[801,805] as intended, the middle of the hydrocarbon chain slots between the side chain of Ile109 and the backbone of Gly172 (Figure 2d).

The conformation of a HBS helix has been previously reported in isolation,[20] but to date this class of molecule has not been crystallized in complex with a target protein. The crystal structure of HBS myoA bound to MTIP demonstrates that the geometry of a HBS constraint is maintained in the complex, providing the first direct structural evidence that this motif organizes the helix in the context of a bound protein target (Figure 2e and f). Markedly lower B-factors in the HBS helix support the hypothesis that the helix is stabilized by the constraint, although CD data suggest only a modest increase in helicity for the isolated peptide (Supplementary Figure S5). Since the HBS constraint is positioned at the N-terminus of the helix, steric clashes of the tether with the congested MTIP binding groove are avoided. These results therefore experimentally support the prediction[6] that the HBS strategy may be suitable for targeting buried helix interactions by remotely reinforcing existing interactions, without interfering with a complex multiface helix binding interface.

Crucially, despite engaging in productive interactions, the pGly staples do not affect the register of the helix as observed, for example, in a (*i*, *i* + 7) stapled p53-Mdm2 complex,[9] and therefore they do not interfere with key protein−helix interactions. These structures further show that when the MTIP clamp forms, the central binding groove becomes highly congested, raising the possibility that replacement of Hα by methyl groups may be unfavorable due to steric hindrance. A modest increase in stability of the complex with MTIP on removal of these α-Me groups in otherwise identical peptides tends to support this hypothesis (Figure 3). For example, the

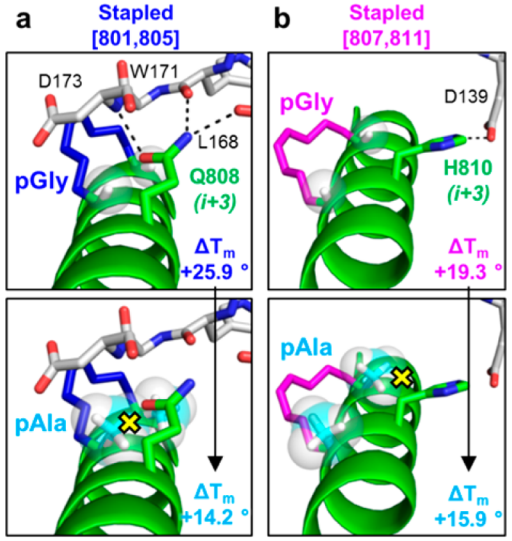

Figure 3. Potential for steric clash (yellow crosses) of pAla staples (modeled in PyMOL; substituents on Cα shown as spheres) with polar *i*+3 residues in a buried protein−helix interaction. The experimental co-crystal structures of MTIP with (a) pGly[801,805] and (b) pGly[807,811] are used as illustrative examples. Shown are the effects on ΔT_m due to substitution at Cα.

side chain amide functionality of Gln808, which makes several polar contacts with the backbone of MTIP at residues Leu168, Trp171, and Asp173, would clash with an α-Me group on the *i*−3 residue in pAla[801,805] (Figure 3a). Similarly, the α-Me at residue 807 in the pAla[807,811] staple may clash with the polar side chain of His810 that engages in a key interaction with Asp139 in the MTIP interdomain linker (Figure 3b). In contrast, pAla[811,815] is the least disruptive pAla staple; in this peptide one *i*+3 residue (Lys814) makes a flexible interaction with the MTIP C-terminus (Gln204), while the other (Gln818) is known to be dispensable. The pGly staples may also allow the peptides to retain a greater degree of flexibility than pAla staples, enabling adoption of an optimal binding conformation. Analysis of the binding of lactam-bridged constrained peptides of the C-terminal heptad repeat of HIV-gp41 showed that a flexible linker served to reduce the number of conformational degrees of freedom available to the unbound peptide, but excessive constraint ran the risk of

dx.doi.org/10.1021/cb500271c | *ACS Chem. Biol.* 2014, 9, 2204−2209

locking the helix in an "inactive" conformation.[21] It is plausible that such interplay is also important in the complexes of different stapled myoA peptides, although in this study we have not undertaken to correlate stapled helix stability with potency. It has been emphasized elsewhere that this correlation is not simple, and a recent debate over such effects in BimBH3 stapled peptides highlights that different properties must be optimized for different experiments to ensure the success of the stapling strategy.[3,22−24]

In summary, we have made the first comparison of three state-of-the-art helix constraint technologies at atomic resolution. Furthermore, we have presented the first examples of stapled and hydrogen bond surrogate (HBS) peptides designed to disrupt a fully buried PPI in which MTIP not only discriminates for polar and nonpolar functionality presented by all faces of the myoA helix but also forms a tight clamp around the ligand to include the helix in its hydrophobic core. We have demonstrated that monosubstituted pentenyl glycine (pGly) staples or an N-terminal HBS motif may be implemented in myoA tail helices without disruption of native side chain interactions or helix register, resulting in several peptides that match or even improve on high WT myoA affinity. Validation of the binding mode by combined structural analysis including three novel high-resolution X-ray structures shows that careful molecular design of the constraints is required for their successful implementation in such complex PPIs. The data presented here will be a useful resource for designing analogous inhibitors, in particular for the diverse range of buried protein−helix interactions found in nature, potentially opening up a new class of PPIs for therapeutic intervention and/or tool development.

■ ASSOCIATED CONTENT

Supporting Information

Experimental details including amino acid and peptide synthesis, X-ray crystallographic analysis, and assay protocols. This material is available free of charge via the Internet at http://pubs.acs.org.

Accession Codes

The structures have been deposited in the Protein Data Bank as PDB entries 4MZJ (MTIP-pGly[801,805] complex), 4MZK (MTIP-pGly[807,811]), and 4MZL (MTIP-HBS myoA).

■ AUTHOR INFORMATION

Corresponding Authors

*E-mail: e.cota@imperial.ac.uk.
*E-mail: e.tate@imperial.ac.uk.

Present Address

[⊥]The Institute of Cancer Research, 15 Cotswold Road, Belmont, Sutton, Surrey SM2 5NG, U.K.

Notes

The authors declare no competing financial interest.

■ ACKNOWLEDGMENTS

We thank the beamline scientists at I02 and I04 of the Diamond Light Source and J. Marchant and I. Pérez-Dorado at the Centre for Structural Biology, Imperial College, for useful discussions. We also thank Pfizer plc for the gift of (*R*)-*N*-Fmoc (4′-octenyl) alanine and members of the Tate group for critical reading of the manuscript. This work was supported by the Institute of Chemical Biology EPSRC Centre for Doctoral Training (studentships to C.H.D. and Y.S.) and the EPSRC (CASE studentship award to J.C.T.).

■ REFERENCES

(1) Azzarito, V., Long, K., Murphy, N. S., and Wilson, A. J. (2013) Inhibition of alpha-helix-mediated protein-protein interactions using designed molecules. *Nat. Chem. 5*, 161−173.

(2) Henchey, L. K., Jochim, A. L., and Arora, P. S. (2008) Contemporary strategies for the stabilization of peptides in the alpha-helical conformation. *Curr. Opin. Chem. Biol. 12*, 692−697.

(3) Walensky, L. D., and Bird, G. H. (2014) Hydrocarbon-stapled peptides: Principles, practice, and progress. *J. Med. Chem.*, DOI: 10.1021/jm4011675.

(4) Kushal, S., Lao, B. B., Henchey, L. K., Dubey, R., Mesallati, H., Traaseth, N. J., Olenyuk, B. Z., and Arora, P. S. (2013) Protein domain mimetics as in vivo modulators of hypoxia-inducible factor signaling. *Proc. Natl. Acad. Sci. U.S.A. 110*, 15602−15607.

(5) Chang, Y. S., Graves, B., Guerlavais, V., Tovar, C., Packman, K., To, K. H., Olson, K. A., Kesavan, K., Gangurde, P., Mukherjee, A., Baker, T., Darlak, K., Elkin, C., Filipovic, Z., Qureshi, F. Z., Cai, H., Berry, P., Feyfant, E., Shi, X. E., Horstick, J., Annis, D. A., Manning, A. M., Fotouhi, N., Nash, H., Vassilev, L. T., and Sawyer, T. K. (2013) Stapled alpha-helical peptide drug development: A potent dual inhibitor of MDM2 and MDMX for p53-dependent cancer therapy. *Proc. Natl. Acad. Sci. U.S.A. 110*, E3445−3454.

(6) Bullock, B. N., Jochim, A. L., and Arora, P. S. (2011) Assessing helical protein interfaces for inhibitor design. *J. Am. Chem. Soc. 133*, 14220−14223.

(7) Raj, M., Bullock, B. N., and Arora, P. S. (2013) Plucking the high hanging fruit: A systematic approach for targeting protein-protein interactions. *Bioorg. Med. Chem. 21*, 4051−4057.

(8) Phillips, C., Roberts, L. R., Schade, M., Bazin, R., Bent, A., Davies, N. L., Moore, R., Pannifer, A. D., Pickford, A. R., Prior, S. H., Read, C. M., Scott, A., Brown, D. G., Xu, B., and Irving, S. L. (2011) Design and structure of stapled peptides binding to estrogen receptors. *J. Am. Chem. Soc. 133*, 9696−9699.

(9) Baek, S., Kutchukian, P. S., Verdine, G. L., Huber, R., Holak, T. A., Lee, K. W., and Popowicz, G. M. (2012) Structure of the stapled p53 peptide bound to Mdm2. *J. Am. Chem. Soc. 134*, 103−106.

(10) Stewart, M. L., Fire, E., Keating, A. E., and Walensky, L. D. (2010) The MCL-1 BH3 helix is an exclusive MCL-1 inhibitor and apoptosis sensitizer. *Nat. Chem. Biol. 6*, 595−601.

(11) Baum, J., Papenfuss, A. T., Baum, B., Speed, T. P., and Cowman, A. F. (2006) Regulation of apicomplexan actin-based motility. *Nat. Rev. Microbiol. 4*, 621−628.

(12) Bergman, L. W., Kaiser, K., Fujioka, H., Coppens, I., Daly, T. M., Fox, S., Matuschewski, K., Nussenzweig, V., and Kappe, S. H. (2003) Myosin A tail domain interacting protein (MTIP) localizes to the inner membrane complex of Plasmodium sporozoites. *J. Cell. Sci. 116*, 39−49.

(13) Bosch, J., Turley, S., Daly, T. M., Bogh, S. M., Villasmil, M. L., Roach, C., Zhou, N., Morrisey, J. M., Vaidya, A. B., Bergman, L. W., and Hol, W. G. (2006) Structure of the MTIP-MyoA complex, a key component of the malaria parasite invasion motor. *Proc. Natl. Acad. Sci. U.S.A. 103*, 4852−4857.

(14) Thomas, J. C., Green, J. L., Howson, R. I., Simpson, P., Moss, D. K., Martin, S. R., Holder, A. A., Cota, E., and Tate, E. W. (2010) Interaction and dynamics of the *Plasmodium falciparum* MTIP-MyoA complex, a key component of the invasion motor in the malaria parasite. *Mol. Biosyst. 6*, 494−498.

(15) Bosch, J., Turley, S., Roach, C. M., Daly, T. M., Bergman, L. W., and Hol, W. G. (2007) The closed MTIP-myosin A-tail complex from the malaria parasite invasion machinery. *J. Mol. Biol. 372*, 77−88.

(16) Douse, C. H., Green, J. L., Salgado, P. S., Simpson, P. J., Thomas, J. C., Langsley, G., Holder, A. A., Tate, E. W., and Cota, E. (2012) Regulation of the *Plasmodium* motor complex: phosphorylation of myosin A tail-interacting protein (MTIP) loosens its grip on MyoA. *J. Biol. Chem. 287*, 36968−36977.

(17) Yeo, D. J., Warriner, S. L., and Wilson, A. J. (2013) Monosubstituted alkenyl amino acids for peptide "stapling". *Chem. Commun. 49*, 9131−9133.
(18) Blackwell, H. E., and Grubbs, R. H. (1998) Highly efficient synthesis of covalently cross-linked peptide helices by ring-closing metathesis. *Angew. Chem., Int. Ed. 37*, 3281−3284.
(19) Nomura, W., Aikawa, H., Ohashi, N., Urano, E., Metifiot, M., Fujino, M., Maddali, K., Ozaki, T., Nozue, A., Narumi, T., Hashimoto, C., Tanaka, T., Pommier, Y., Yamamoto, N., Komano, J. A., Murakami, T., and Tamamura, H. (2013) Cell-permeable stapled peptides based on HIV-1 integrase inhibitors derived from HIV-1 gene products. *ACS Chem. Biol. 8*, 2235−2244.
(20) Liu, J., Wang, D., Zheng, Q., Lu, M., and Arora, P. S. (2008) Atomic structure of a short alpha-helix stabilized by a main chain hydrogen-bond surrogate. *J. Am. Chem. Soc. 130*, 4334−4337.
(21) Sia, S. K., Carr, P. A., Cochran, A. G., Malashkevich, V. N., and Kim, P. S. (2002) Short constrained peptides that inhibit HIV-1 entry. *Proc. Natl. Acad. Sci. U.S.A. 99*, 14664−14669.
(22) Okamoto, T., Zobel, K., Fedorova, A., Quan, C., Yang, H., Fairbrother, W. J., Huang, D. C. S., Smith, B. J., Deshayes, K., and Czabotar, P. E. (2013) Stabilizing the pro-apoptotic BimBH3 Helix (BimSAHB) does not necessarily enhance affinity or biological activity. *ACS Chem. Biol. 8*, 297−302.
(23) Bird, G. H., Gavathiotis, E., LaBelle, J. L., Katz, S. G., and Walensky, L. D. (2014) Distinct BimBH3 (BimSAHB) stapled peptides for structural and cellular studies. *ACS Chem. Biol. 9*, 831−837.
(24) Okamoto, T., Segal, D., Zobel, K., Fedorova, A., Yang, H., Fairbrother, W. J., Huang, D. C. S., Smith, B. J., Deshayes, K., and Czabotar, P. E. (2014) Further insights into the effects of pre-organizing the BimBH3 helix. *ACS Chem. Biol. 9*, 838−839.